Eur. Phys. J. D **42**, 317–324 (2007)
DOI: 10.1140/epjd/e2007-00052-6

THE EUROPEAN PHYSICAL JOURNAL D

Feasibility of narrow-line cooling in optical dipole traps

Ch. Grain[1], T. Nazarova[1], C. Degenhardt[1,a], F. Vogt[1], Ch. Lisdat[2], E. Tiemann[2], U. Sterr[1,b], and F. Riehle[1]

[1] Physikalisch-Technische Bundesanstalt, Bundesallee 100, 38116 Braunschweig, Germany
[2] Institut für Quantenoptik, Leibniz Universität Hannover, Welfengarten 1, 30167 Hannover, Germany

Received 12 September 2006 / Received in final form 19 February 2007
Published online 9 March 2007 – © EDP Sciences, Società Italiana di Fisica, Springer-Verlag 2007

Abstract. We have investigated the influence of narrow-line laser cooling on the loading of Ca atoms into optical dipole traps. To describe the narrow-line cooling of alkaline-earth atoms in combination with optical dipole trapping, we have developed a model that takes into account the light shifts of the cooling transition in three dimensions. The model is compared with two experimental realizations of optical dipole traps for calcium at the wavelengths 514 nm and 10.6 μm.

PACS. 32.80.Pj Optical cooling of atoms; trapping – 32.60.+i Zeeman and Stark effects – 32.80.Lg Mechanical effects of light on atoms, molecules, and ions

1 Introduction

Optical dipole traps and optical lattices have become indispensable tools for applications such as Bose-Einstein condensation (BEC) [1–3], optical clocks [4], single atom manipulation [5], quantum information processing [6,7], and photoassociation spectroscopy [8], to name only a few. For most of these applications it is mandatory to transfer laser-cooled atoms with high efficiency into a dipole trap.

For alkaline elements efficient sub-Doppler laser cooling techniques can be employed that in general also work under the conditions of an optical dipole trap. Thus the dipole trap can be combined with a magneto optical trap (MOT) which leads to a good transfer of atoms from the MOT to the dipole trap with efficiencies in the order of 40% [9].

Atoms with a single nondegenerate ground state $^1S_0$ and with no nuclear spin like the most abundant isotopes of Mg, Ca, Sr or Yb cannot be cooled by the usual sub-Doppler techniques mentioned above. On the other hand, these atoms exhibit almost forbidden transitions making them especially interesting as optical frequency standards, for atom interferometry, cold collisions studies or for possible creation of a BEC by all optical means. Doppler cooling on these forbidden transitions [10], eventually using an additional quench laser beam to increase the scattering force [11,12], can also lead to temperatures in the range of a few μK and below [13–15].

To acquire a better understanding of the cooling process and the loading mechanisms for these species in conjunction with an optical dipole trap we developed a model for narrow-line cooling in an optical dipole trap. From the model a completely different behavior is predicted, whether the narrow-line cooling transition is shifted to the blue or to the red by the ac-Stark effect, depending on the wavelength of the trapping laser. This is different from the alkaline elements, where the ground and excited state are always shifted in opposite directions, thus in an attractive potential for ground state atoms, the broad cooling transition becomes shifted to the blue. We have experimentally investigated these predictions with two kinds of dipole traps and narrow-line cooled Ca atoms. In the first one, a 514 nm Ar^+ laser with 8.6 W power is used to create an optical trap with a depth of about 50 μK. In the second kind, a CO_2 laser emitting 80 W at 10.6 μm is used to create a similar potential depth. These two cases correspond to the blue and red shifted case as mentioned above. We observed an increase in the trapping efficiency with increasing temporal overlap between the narrow-line MOT and the 514 nm trap. In the second case with the CO_2 trap, atoms could only be trapped when there was no temporal overlap between the MOT and the dipole trap.

After a brief overview of the cooling and trapping scheme used in our experiment in Section 2, we will describe the basics of optical dipole trapping and the model for laser cooling in a dipole trap in Section 3. Then, in Section 4 we will present the experimental setup and the results for trapping of ultracold Ca atoms in both kinds of optical dipole traps.

2 Narrow-line cooling

Narrow-line cooling differs from usual Doppler cooling on strongly allowed transitions by the fact, that the

[a] *Present address*: Philips Research Laboratories, 52066 Aachen, Germany.
[b] e-mail: uwe.sterr@ptb.de

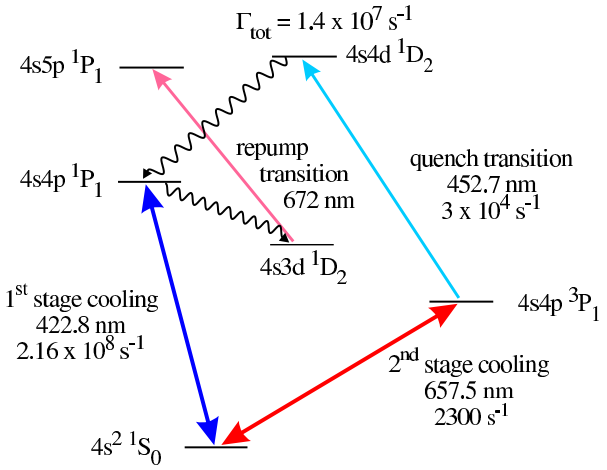

Fig. 1. Energy levels and optical transitions involved in laser cooling of calcium. Transition wavelengths and corresponding Einstein A-factors are shown.

linewidth Γ of the cooling transition is smaller than the change in the Doppler shift induced by a single photon recoil, i.e. $\Gamma < \hbar k^2/M$, where M is the atomic mass and k the wave vector of the exciting light. Thus, a single spontaneous photon can make a significant difference in the Doppler-shift and in the absorption rate. In the case of a monochromatic excitation, a single spontaneous emission can bring an atom out of resonance. Therefore, individual absorption and emission events have to be taken into account and usually a multichromatic excitation spectrum is used to access a broad velocity distribution, where the upper edge of this frequency spectrum is detuned about one linewidth below the atomic resonance. In this case, calculations predict a minimum temperature well below the recoil limit [10].

This cooling scheme yields a maximum force $F_{\max} = \hbar k \Gamma/2$. For very narrow lines, e.g. the calcium intercombination line $^1\mathrm{S}_0 - ^3\mathrm{P}_1$ with $\Gamma = 2300\ \mathrm{s}^{-1}$ the force $F_{\max}$ is only 1.5 times the gravitational force. To increase the force the lifetime of the upper level can be reduced by exciting the transition to the $4s4d\ ^1\mathrm{D}_2$ state ($\lambda = 453$ nm), Figure 1. From this state atoms decay rapidly via the $4s4p\ ^1\mathrm{P}_1$ level to the ground state [16]. Solving the optical Bloch equations of this system leads to an effective two level system with an effective linewidth of $\Gamma_{\mathrm{eff}} = \Gamma + r_{12}$ where r_{12} is the quenching rate [11]. Hence, artificially reducing the lifetime (quenching) of the upper level of the narrow transition by exciting a third level, which quickly decays to the ground state, makes narrow-line cooling possible on a wide range of linewidths.

In difference to usual sub-Doppler mechanisms that rely on slow, velocity dependent evolutions of coherences in the ground states [17,18], narrow-line cooling relies on the Doppler shift of an optical transition. Thus it is very sensitive to level shifts, which can have severe implications when this scheme is employed inside an optical dipole trap.

3 Optical dipole traps

One very simple way to trap neutral atoms is the use of a strongly focused Gaussian laser beam [19,20] where the electrical field $\boldsymbol{E}$ of the laser beam induces a dipole moment $\boldsymbol{P}$ in the atom. The interaction of this dipole moment with the external field gives rise to the potential $U = -\frac{1}{2}\langle \boldsymbol{P} \cdot \boldsymbol{E} \rangle$ where the brackets denote a temporal average. For a laser beam with an amplitude of the electric field $E(\boldsymbol{r})$, a frequency $\nu = \omega/2\pi$ and a polarization p interacting with the Zeeman sub-level m_i of an atomic state i, the potential due to the ac-Stark shift $U_i(\omega, p, m_i, \boldsymbol{r})$ can be calculated in second-order perturbation theory [21]. The shift U_i can be written as a function of the product of the intensity I and the normalized ac-Stark level shift κ (Fig. 2)

$$U_i(\omega, p, m_i, \boldsymbol{r}) = h\kappa_i(\omega, p, m_i) I(\boldsymbol{r}) \tag{1}$$

where the normalized ac-Stark shift can be calculated as

$$\kappa_i(\omega, p, m_i) = -\frac{3\pi c^2}{h} \sum_{k, m_k} \frac{A_{ki}(2J_k + 1)}{\omega_{ik}^2(\omega_{ik}^2 - \omega^2)} \begin{pmatrix} J_i & 1 & J_k \\ -m_i & p & m_k \end{pmatrix}^2 \tag{2}$$

with the sum taken over all states k coupled to the state of interest i by transitions with Einstein coefficients A_{ki} and frequencies ω_{ik} [22]. J_i and J_k are the total angular momenta of the states i and k, and the expression in the large brackets denotes a $3J$-symbol [23].

Close to the potential minimum $U(0) = -U_0$ the trapping potential of a focused Gaussian beam can be approximated by a harmonic potential

$$U(r, z) \simeq -U_0 \left[1 - 2\left(\frac{r}{w_0}\right)^2 - \left(\frac{z}{z_{\mathrm{R}}}\right)^2 \right] \tag{3}$$

with the waist radius w_0 and the Rayleigh length $z_{\mathrm{R}} = \pi w_0^2/\lambda$. In this case the frequencies of the radial and the axial harmonic motion of an atom with mass M are

$$\omega_{\mathrm{rad}} = \sqrt{\frac{4U_0}{M w_0^2}},\ \omega_{\mathrm{ax}} = \sqrt{\frac{2U_0}{M z_{\mathrm{R}}^2}}, \tag{4}$$

respectively.

3.1 Cooling in an optical dipole trap

To reach high phase-space densities in an optical dipole trap, atoms from the MOT have to be transferred to the dipole trap with high efficiency. Once there is a sufficient number of atoms accumulated in the trap, several ways are available for further increase of phase space density like sideband cooling [24] in an optical lattice or evaporative cooling [25,26].

The optimum size of the dipole trap for best transfer at a given available power is discussed in detail in [27] and references therein. It turns out that for a trap depth bigger than four times the thermal energy of the laser-cooled

atoms, the number of trapped atoms becomes nearly independent of the trap depth. Thus the acceptable size of the trapping laser beam of the dipole trap at a given atomic temperature is determined by the available optical power, and then in most dipole traps, the size of the trapping region is smaller than the initial size of the MOT. As the trap is conservative, without any additional dissipation mechanisms or thermalizing collisions, atoms that cross the dipole trap will not become trapped, but immediately leave the trapping potential. This limits the number of trapped atoms to those atoms that were already present at the position of the dipole trap when it was turned on, and that had sufficiently small kinetic energy to remain trapped, i.e. the fraction is determined from the overlap of the initial phase space volume with the phase space volume that is trapped in the dipole trap [28]. Thus, to efficiently transfer atoms from the MOT to the dipole trap, a dissipation mechanism is required that is usually provided through laser cooling by the MOT beams. Then during the simultaneous operation of the MOT and the dipole trap, the number of atoms captured in the dipole trap will increase with time, until other loss mechanisms prevail.

As example we consider the case of the Ar^+ laser trap for calcium with a beam waist of $w_0 = 100$ μm and potential depth $U_0 = 45$ $\mu\mathrm{K} \times k_\mathrm{B}$ oriented along x that is superimposed to a MOT with rms radius $\sigma_i \approx 400$ μm ($i = x, y, z$) and sample temperature $T = 16$ μK (rms velocity of $v_\mathrm{rms} = 10$ cm/s). The potential of the dipole trap is 2.8 times deeper than the kinetic energy and atoms up to a radius of $r_\mathrm{eff} \approx 0.56\, w_0$ from the center have an average kinetic energy $(3/2)\, k_\mathrm{B}T$ less than the local potential depth. The corresponding cross section of the dipole trap $A_\mathrm{dip} \approx \pi r_\mathrm{eff}^2$ is approximately 100 times smaller than the cross section of the MOT $A_\mathrm{MOT} \approx 2\pi\sigma_y\sigma_z$ and the fraction of atoms that are trapped initially without further laser cooling amounts to less than 1%. For atoms in the surrounding MOT, it takes about 10 ms to make a round trip in the MOT. From the ratio of the cross sections, on about every 100th round trip, i.e. on average after 1 s, the atom passes through the dipole trap within a transit time of about $2w_0/v_\mathrm{rms} \approx 2$ ms. Thus, to load the dipole trap with these atoms, the cooling mechanism must remove the kinetic energy and decelerate the atom during this short transit time. It is therefore essential that the narrow-line cooling inside the dipole trap works as efficiently as in free space [29]. If this is the case in our present example, Ca atoms would absorb during the transit time through the dipole trap around 20 photons of the 657 nm radiation, which grants a sufficient cooling to trap the atoms in the dipole trap.

However, as narrow-line cooling critically depends on the detuning between the cooling laser and the atomic transition, the influence by the ac-Stark shift on the wavelength needs to be considered. Figure 2 shows the normalized level shifts $\kappa(\lambda)$ as a function of the wavelength λ. There are wavelengths where the ac-Stark shift of the ground state is equal to the ac-Stark shift of one of the Zeeman sublevels of the excited state. Dipole trapping at

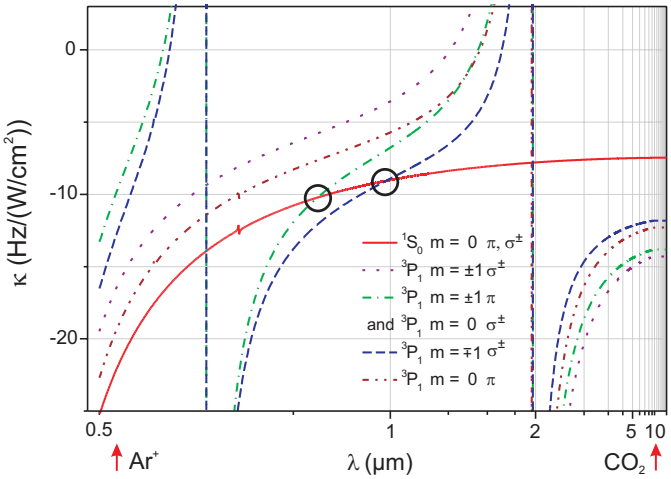

Fig. 2. (Color online) The ac-Stark shift for different polarizations of the trapping laser with intensity of 1 W/cm^2 as a function of its wavelength λ for the calcium $^1\mathrm{S}_0$ ground state and all sublevels of the $^3\mathrm{P}_1$ state. The magic wavelengths are indicated by the two circles. The vertical lines are due to poles in the polarizability from the transition $4s4p\ ^3\mathrm{P}_1 - 4s4d\ ^3\mathrm{D}_{1,2}$ at 1.9 μm and $4s4p\ ^3\mathrm{P}_1 - 4s5s\ ^3\mathrm{S}_1$ at 612 nm.

these so-called "magic wavelengths" could permit to trap the atoms and manipulate them like if they were in free space [13]. An alternative way to overcome this situation was presented in [30] by engineering the light-shift using an auxiliary laser field.

One zero-crossing for the $m_\mathrm{S} = 0 - m_\mathrm{P} = \pm 1$ transition and π-polarized dipole laser or $m_\mathrm{S} = 0 - m_\mathrm{P} = 0$ transition and $\sigma^\pm$-polarized dipole laser lies at 800.8 nm. A second zero-crossing for the $m_\mathrm{S} = 0 - m_\mathrm{P} = \mp 1$ transition and $\sigma^\pm$-polarized dipole laser is at 983 nm [21].

When the optical dipole trap is superimposed to a MOT, however, because of the spatially varying magnetic fields and the 3D laser configuration the magic wavelength cannot be realized everywhere in the dipole trap and for all cooling laser beams. We therefore have simulated quench-cooling in a dipole trap, taking into account the light shifts of the cooling transition due to the dipole laser and the magnetic field of the MOT. A rate equation model for quench cooling in free space and in a MOT [31] was modified to include the level shifts in the optical dipole trap. The effect of the light field of the dipole laser on the energies of the individual sublevels of the $^3\mathrm{P}_1$ and the $^1\mathrm{D}_2$ level is described according to equation (2) using a decomposition into scalar, vectorial, and tensorial parts. For the simultaneous action of the magnetic and the electric field, the full Hamiltonian is diagonalized at each point in the trap to give the total shift of the individual Zeeman levels (Fig. 3).

Depending on the relative shift between the ground state and the excited states we can distinguish two limiting cases. In case (a), that is realized with an Ar^+ trap, the light shifts of all excited states are smaller than the shift of the ground state (Fig. 3a). Outside the dipole trap, the spectrum of the cooling laser is detuned below the atomic resonance. Because of the differential light shifts, inside

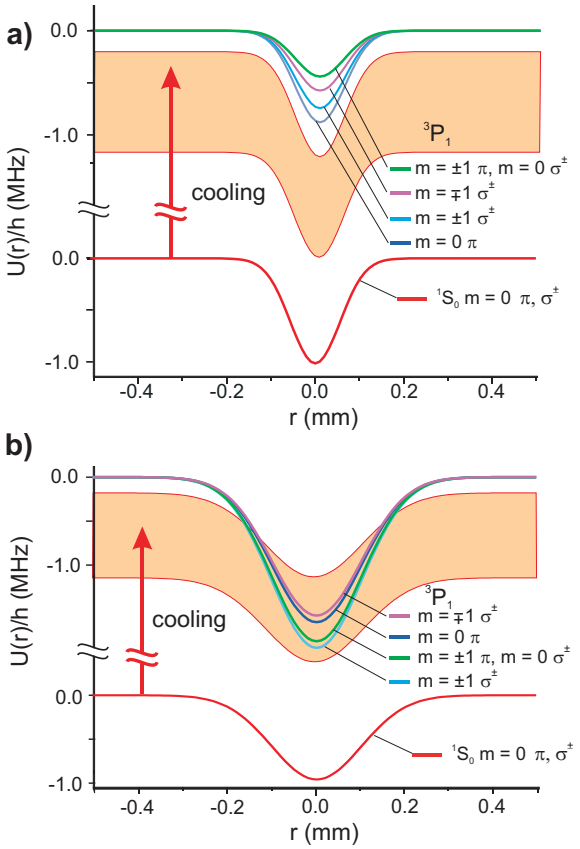

Fig. 3. (Color online) The ac-Stark shifts as a function of the radial distance r to the center of the dipole trap without additional magnetic fields. On the top for case (a), e.g. for an Ar^+ laser trap ($\lambda = 514$ nm) and on the bottom for case (b), e.g. a CO_2 laser trap ($\lambda = 10.6$ μm). The broadened spectrum of the cooling laser is indicated by the band.

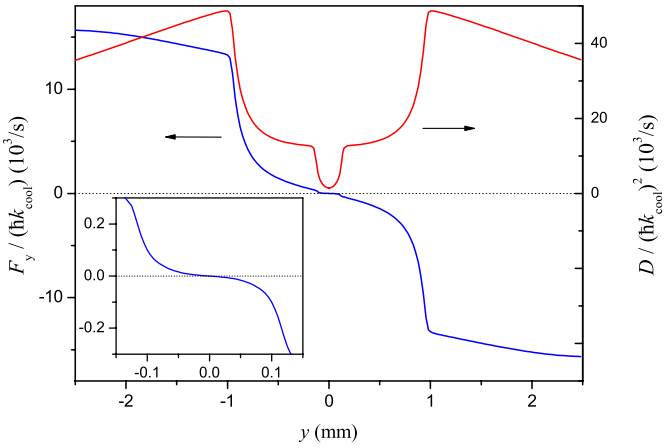

Fig. 4. (Color online) Narrow-line cooling force F_y and diffusion rate D in units of 657 nm photon momenta $p_{rec} = \hbar k_{cool}$ per second for atoms at rest as a function of the radial atomic position (along the y-axis) inside the 514 nm Ar^+ laser trap. The dipole trap beam is oriented along the x axis and polarized along the z-direction with power $P = 8$ W and waist radius $w_0 = 110$ μm. The insert shows a zoom of the central part of the force curve.

the trap the spectrum remains red detuned. Thus, cooling forces, i.e. velocity dependent, dissipating light forces are still present even at the center of the dipole trap. As inside the trap the detuning is increased, we expect a slight decrease of the cooling efficiency.

In the second case (b) opposite to (a), the light shift of the excited states is larger than the one of the ground state. Experimentally this case is realized e.g. in a CO_2 trap ($\lambda = 10.6$ μm). In this case the spectrum of the cooling laser, that is detuned below the atomic resonance outside the trap is shifted into resonance when the atom enters the dipole trap (Fig. 3b). Thus the absorption rate no longer depends on the atomic velocity and no damping of the atomic motion can occur. Instead, the increased resonant scattering on the narrow line and on the quench transition leads to heating due to the random photon recoil.

The effect of the differential light shift on the narrow-line cooling can be seen more quantitatively in the light forces and diffusion rates due to the absorption of the narrow-line cooling laser and the quench laser. First the level shift and the atomic eigenstates of the $^1S_0$ ground state, the intermediate $^3P_1$ state of the cooling process, and the $^1D_2$ quench state (Fig. 1) due to the combined electric field of the dipole trap and the magnetic quadrupole field of the MOT are calculated. For simplicity we have neglected the ac-Stark shift of the quench transition but still considered its influence on the absorption probability for the different polarizations of the 6 quench laser beams. With the resulting eigenstates the excitation rates from each cooling and quenching beam according to its polarization and detuning are calculated. From these rates the steady-state absorption rates and position and velocity dependent average light forces were calculated. The heating rate

$$(dE/dt)_{heat} = \hbar^2 k_{cool}^2 R_{cool}/m + \hbar^2 k_q^2 R_q/m = D/m \quad (5)$$

and the momentum diffusion constant D due to spontaneous emission [32] are calculated from the rates R_{cool} for emission from the $^3P_1$ state and R_q for emission from the $^1D_2$ state after the quenching.

In the simulation a power of 4.7 mW in a beam radius $w_{laser} = 2.4$ mm for each of the horizontal 657 nm cooling laser beams and 8.7 mW in a beam radius $w_{laser} = 2.4$ mm for the vertical beams was used. The 657 nm laser is assumed to have a rectangular spectrum with width 1.4 MHz and the upper edge detuned by 140 kHz below the atomic line. For each of the 6 quench laser beams a power of 70 mW in a beam radius of 4.6 mW was used. These laser fields (6 cooling beams, 6 quenching beams, and the dipole trap laser beam) and their polarizations were described in close agreement with the values of the real experiment.

Figures 4 and 5 show the profiles of the narrow-line cooling force F_y for atoms at rest in a direction perpendicular to the axis of the Ar^+ laser dipole trap and the CO_2 laser trap respectively. For distances $r > 0.3$ mm, larger than the radii of the dipole traps, the force acts toward the trap center. The dependence on the radial direction is due to the spectrum of the cooling beam and the

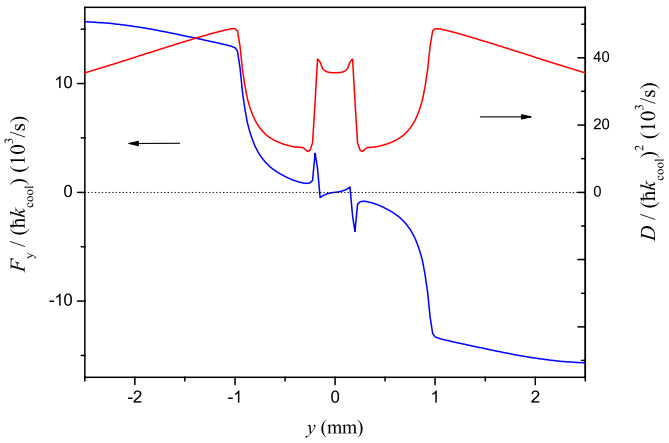

Fig. 5. (Color online) Narrow-line cooling force F_y and diffusion rate D in units of 657 nm photon momenta $p_{rec} = \hbar k_{cool}$ per second for atoms at rest as a function of the radial atomic position (along the y-axis) inside the 10.6 μm CO_2 laser trap. The dipole trap beam is propagating along the x-axis and polarized along the z-direction with power $P = 80$ W and waist radius $w_0 = 220$ μm.

effective linewidth of the cooling transition. At a radius of $r \approx 1$ mm the blue edge of the rectangular cooling laser spectrum is shifted into resonance by the magnetic field.

In both cases the dipole trap strongly modifies the spatial dependency of the force, as inside the dipole trap the quantization axis is determined by the dipole laser field and no longer by the magnetic quadrupole field of the MOT. Thus the spatially restoring force of the MOT is no longer present inside the dipole trap, but is replaced by the much stronger dipole forces that are not shown in both figures. The main difference between both cases is in the diffusion constant D i.e. the rate of spontaneous emission: in the Ar^+ trap the coefficient is close to zero inside the trap, while in the CO_2 trap significant diffusion is present inside the dipole trap that is not compensated by a restoring force (in momentum space as well).

4 Experimental results

Experimentally the two cases of narrow line cooling in an optical dipole trap discussed in Section 3.1 were studied at two wavelengths detuned far away from any atomic resonances. Case (a) was studied with a 514 nm Ar^+ laser trap and case (b) with a 10.6 μm CO_2 laser trap. The two experimental realizations were performed in two slightly different vacuum chambers but using the same two-stage cooling method to prepare the initial sample of ultracold atoms.

4.1 Preparation of the ultra-cold sample

In a first cooling stage atoms were captured from an atomic beam and cooled to millikelvin temperatures by use of a standard MOT based on the broad 423 nm transition (Fig. 1). For the first stage cooling about 500 mW of 423 nm light from a frequency-doubled Ti:sapphire laser was used. A small loss channel due to small fraction of excited atoms on the cooling transition decaying to an intermediate long lived state $^1D_2$ was closed by use of a repump laser at 672 nm (Fig. 1). In the case of the Ar^+ laser dipole trap the MOT was loaded directly from the low-velocity part of a thermal atomic beam. Later in the CO_2 trap a Zeeman slower was used to increase the number of atoms in the thermal beam with velocities slower than 30 m/s that can be trapped by the 423 nm MOT. As the ground state is non-degenerate, the lowest temperature that can be achieved on this transition is about a factor of 3 above the Doppler limit $T_D = \hbar\Gamma/2k_B \approx 800$ μK.

In the second cooling stage the narrow transition $^1S_0 - ^3P_1$ was used for Doppler cooling. To increase the scattering rate, the lifetime in the excited state was reduced by optical pumping to the $^1D_2$ state by an additional 453 nm laser. With the available power in the quench laser beam an effective linewidth $\Gamma_{eff} = 2\pi \times 5$ kHz was obtained, which is smaller than the recoil shift $\delta_{rec} = 2\pi \times 11.6$ kHz. To avoid a loss of atoms due to the random recoil and to increase the capture range the excitation spectrum of the red light was broadened by a sinusoidal frequency modulation (peak-to-peak amplitude $\delta f_{pp} = 1.4$ MHz, modulation frequency $f_{mod} = 15$ kHz) using an acousto-optic modulator. The high-frequency edge of this frequency comb was detuned below resonance by $\Delta \approx 2\pi \times 120$ kHz.

In the experiment with the Ar^+ dipole trap, from an initial number of $3{\times}10^7$ atoms at 2 mK that were loaded in 300 ms during the first cooling stage, up to 35% were transferred to the microkelvin ensemble. After 20 ms of second stage cooling atoms reached temperatures below 10 μK in a cloud of rms-radius of $\sigma_x \approx \sigma_y \approx 0.35$ mm and $\sigma_z \approx 0.24$ mm.

During the CO_2 laser trap experiment after a cooling time of 800 ms in the 423 nm MOT we obtained $\approx 2.5 \times 10^8$ atoms at 2 mK and following 40 ms of cooling in the 657 nm MOT about 4×10^7 atoms were obtained at a temperature of $T \approx 12$ μK.

4.2 Ar^+ laser optical trap

An optical dipole trap corresponding to case (a) of Section 3.1, where the cooling transition stays red detuned from the cooling laser inside the dipole trap was realized by an 514 nm Ar^+ laser. The laser beam with maximum power $P = 8.6$ W was focused to a waist $w_0 = 110$ μm to create a trap of depth of up to $U_0 \approx 50$ $\mu K \times k_B$. The number of atoms was determined from absorption images of the atoms which were obtained by illuminating the trap during 50 μs with a collimated, expanded laser beam tuned to the $^1S_0 - ^1P_1$ transition at 423 nm and imaging the shadow onto a CCD camera (see Fig. 6).

In the Ar^+ trap, the ac-Stark shifts induced by the 514 nm radiation on the ground state and on the excited states are roughly comparable. The net shift of the

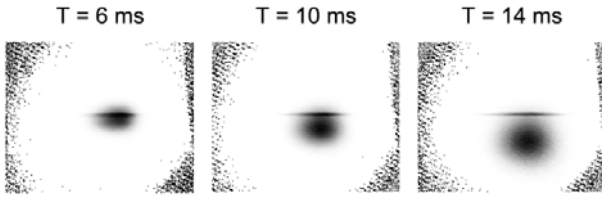

Fig. 6. Absorption images of the calcium atoms for different times T after turning off the MOT, showing atoms trapped in the Ar^+ laser beam and the expanding cloud of untrapped atoms falling down under the influence of gravity. The size of each image is 7 mm × 5.5 mm.

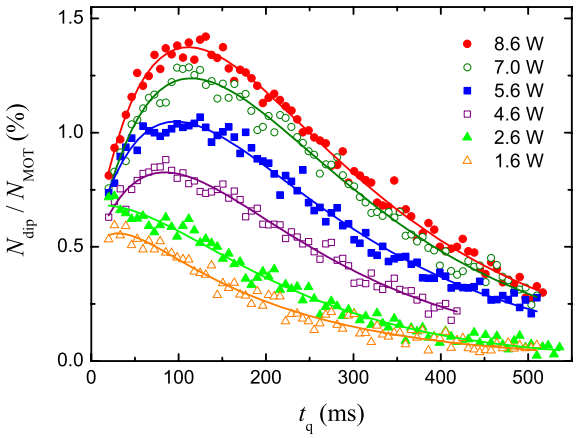

Fig. 7. (Color online) Transfer efficiency $N_{\rm dip}(t_q)/N_{\rm MOT}(0)$ of Ca atoms from the MOT to the Ar^+ laser trap as function of the temporal overlap t_q between MOT and dipole trap for different powers of the dipole beam. The curves show fits according to equation (11).

657 nm cooling transition $^1S_0$–$^3P_1$ that is induced by the σ-polarized 514 nm dipole trap laser beam [21] between +200 kHz and +500 kHz was measured. Thus the cooling laser spectrum remains red detuned from the atomic resonance for all Zeeman components of the cooling transition. Therefore, in agreement with the results of Section 3, when the second stage cooling and the Ar^+ laser trap were overlapped in time we observed an increase of atoms trapped in the dipole trap for increasing overlap time $t_{\rm q}$ (Fig. 7). For times $t_{\rm q} > 100$ ms the loss due to collisions with hot atoms from the background gas and from the thermal atomic beam again reduces the number of trapped atoms. A similar lifetime was obtained for the number of atoms in the surrounding MOT. At maximum about 2% of the atoms could be transferred from the 657 nm MOT to the dipole trap.

We modeled the transfer from the MOT to the dipole trap with the differential equation [9]:

$$\frac{\rm d}{{\rm d}t}N_{\rm dip}(t) = -\frac{1}{\tau_{\rm dip}}N_{\rm dip}(t) + \frac{1}{\tau_{\rm load}}N_{\rm MOT}(t) \qquad (6)$$

where $\tau_{\rm dip}$ is the lifetime of the dipole trap and $\tau_{\rm load}$ the time constant of the loading to the dipole trap. Here any loss of trapped atoms back to the MOT is neglected. For the MOT we assume that the loss due to loading in the dipole trap is negligible, so the number of atoms is:

$$N_{\rm MOT}(t) = N_{\rm MOT}(0)e^{-t/\tau_{\rm MOT}} \qquad (7)$$

where $\tau_{\rm MOT}$ is the lifetime of the MOT. Substituting equation (7) in equation (6) and integrating gives:

$$\frac{N_{\rm dip}(t)}{N_{\rm MOT}(0)} = re^{-t/\tau_{\rm dip}}\left(e^{t/r\tau_{\rm load}} + C_0 - 1\right) \qquad (8)$$

with

$$r = \frac{\tau_{\rm MOT}\tau_{\rm dip}}{\tau_{\rm load}(\tau_{\rm MOT} - \tau_{\rm dip})} \qquad (9)$$

and

$$C_0 = \frac{N_{\rm dip}(0)}{rN_{\rm MOT}(0)}. \qquad (10)$$

If the lifetimes of the MOT $\tau_{\rm MOT}$ and of the dipole trap $\tau_{\rm dip}$ are both limited by the same physical processes and if no extra-heating occurs during the loading of the dipole trap we can assume $\tau_{\rm MOT} \approx \tau_{\rm dip}$ which we also have verified experimentally. Then we obtain for the transfer efficiency:

$$\frac{N_{\rm dip}(t)}{N_{\rm MOT}(0)} = e^{-t/\tau_{\rm dip}}\left(\frac{t}{\tau_{\rm load}} + \frac{N_{\rm dip}(0)}{N_{\rm MOT}(0)}\right), \qquad (11)$$

where $N_{\rm dip}(t)$ denotes the number of atoms trapped in the dipole trap, $N_{\rm MOT}(0)$ the number of atoms trapped in the 657 nm MOT, and $N_{\rm dip}(0)$ the number of atoms in the dipole trap at the time $t = 0$ when the dipole trap is superimposed to the MOT. As shown in Figure 7 this model is in good agreement with the experimental results. The loading time constants $\tau_{\rm load}$ range from $\tau_{\rm load} = 4.4$ s at a dipole laser power of $P = 8.6$ W to $\tau_{\rm load} = 7.7$ s at $P = 4.6$ W.

The loading time constants $\tau_{\rm load}$ that have been fitted to the data of Figure 7 are shown in Figure 8 in comparison with the results of a Monte-Carlo simulation of the loading. We find a good qualitative agreement, however the

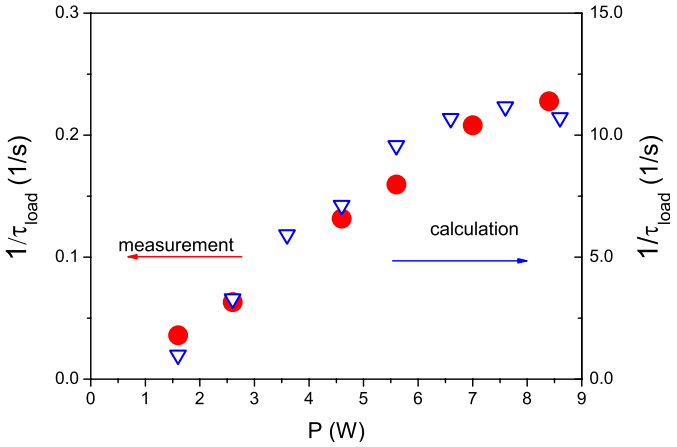

Fig. 8. (Color online) Comparison of the measured loading rates (circles, left scale) and the results of a Monte-Carlo simulation (triangles, right scale).

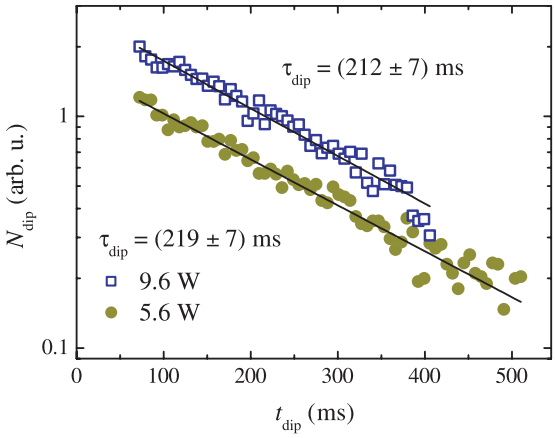

Fig. 9. (Color online) Number of a atoms trapped in the Ar^+ laser trap as a function of trapping time.

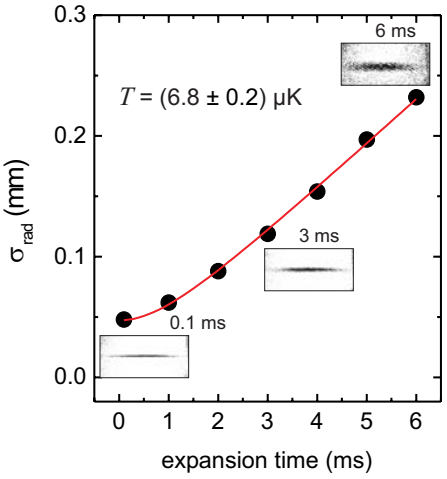

Fig. 10. Expansion of the ultra-cold cloud of Ca atoms released from the Ar^+ laser trap.

simulation predicts rates, that are about a factor 50 bigger than the ones observed. We attribute this large difference to imperfections in the experimental setup compared to the idealized simulation. E.g. the simulation leads to a lower temperature and smaller trap size compared to the experiment and both parameters are drastically changing the loading rate. Experimentally we also observe indications of a density limited MOT size, which we attribute to two-body effects that are not included in the simulation and could be responsible for the differences.

To determine the lifetime of the dipole trap, we record the decay of the number of atoms trapped in the Ar^+ laser beam after the MOT is turned off (Fig. 9). We have observed a lifetime with this optical dipole trap around 210 ms (Fig. 9), independent of the power of the dipole laser. We assume that the small value of the lifetime is due to the collisions with hot atoms, mainly coming directly from the thermal beam.

The temperature of the trapped atoms was measured from the expansion of the atomic cloud after releasing it from the dipole trap. For a thermal velocity distribution with temperature T and initial size $\sigma_{\rm rad}(0)$ the radius of the cloud after an expansion time t is given by

$$\sigma_{\rm rad}(t) = \sqrt{\sigma_{\rm rad}^2(0) + \frac{k_{\rm B}T}{m_{\rm Ca}}t^2}. \qquad (12)$$

Figure 10 shows the rms size $\sigma_{\rm rad}$ of the atomic cloud released from the Ar^+ laser trap along the radial direction and the fitted data that yield a temperature of $T = 6.8\ \mu$K. As the diffusion coefficients and the damping coefficients crucially depend on the atomic position inside the dipole trap, the temperature cannot be directly calculated from them. However the observed temperature is in good agreement with the result from the Monte-Carlo simulation.

4.3 CO_2 laser optical trap

A CO_2 laser emitting at 10.6 μm was used to investigate narrow-line cooling in an optical dipole trap under the conditions of case (b) (Sect. 3.1). CO_2 lasers are known to be very stable in intensity and frequency, resulting in low laser-noise induced heating, which is the dominant heating mechanisms in atom dipole traps [33], and can be easily operated at very high intensities. Furthermore, CO_2 lasers emit at wavelengths far detuned from any molecular transition, which makes CO_2 lasers well suited to trap atoms as well as molecules [34,35]. The CO_2 radiation was delivered by a commercial CO_2 laser. About 80 W of 10.6 μm laser radiation was focused to a waist $w_0 = 220\ \mu$m, resulting in a trap depth of $U_0 = 40\ \mu{\rm K} \times k_{\rm B}$.

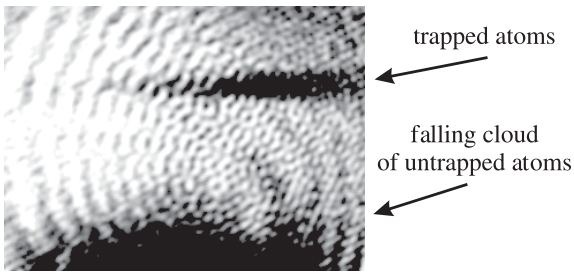

Fig. 11. Absorption picture taken 35 ms after turning off the MOT. It shows the calcium atoms trapped in the CO_2 laser beam and the untrapped atoms falling down. The image corresponds to a region of 7.2 mm× 5.3 mm.

According to the model of Section 3.1 the ac-Stark shift in the CO_2 laser trap leads to a shift of the cooling laser of the MOT toward resonance. Thus it is expected that it will be difficult to load atoms efficiently into the CO_2 trap during the operation of the MOT. Atoms being trapped in the dipole trap are evaporated out of the dipole trap by the resonant excitation from the MOT laser beams. This prediction is confirmed experimentally, since no trapped atoms could be observed when there was a temporal overlap between MOT and dipole trap. Only when the CO_2 trap was switched on immediately after the end of the second stage cooling about 10^5 trapped atoms could be observed in the absorption image (Fig. 11), corresponding to a transfer efficiency from the 657 nm MOT to the CO_2 dipole trap of around 0.3% in

agreement with a Monte-Carlo simulation that simulates the motion of atoms in the potential of the dipole trap without any additional laser cooling. The initial velocity and position is taken randomly from a Gaussian spatial and velocity distribution as in the real MOT. The fraction 0.3% of trapped atoms is determined by the overlap between the phase-space of trapped atoms in the CO_2 laser beam and the atomic ensemble in the 657 nm MOT of size $\sigma_x = \sigma_y = 0.5$ mm and $\sigma_z = 0.7$ mm.

5 Summary

We have investigated narrow-line cooling inside an optical dipole trap in two different regimes. Depending on the sign of the ac-Stark shift of the cooling transition inside the dipole trap, different loading characteristics are expected. The two cases have been realized experimentally in a 514 nm Ar^+ and a 10.6 μm CO_2 laser trap and the predicted behavior has been observed. Efficient loading of an optical trap is very difficult, when the cooling laser is no longer red detuned from the narrow-line cooling transition inside the trap. From our model, we expect to obtain best transfer efficiencies, if the dipole trap is operated close to the magic wavelength of 983 nm. In this case one Zeeman component of the cooling transition is not shifted by the dipole trapping fields, and thus laser cooling similar to free space will be possible. All other Zeeman components are shifted away from resonance, so no additional heating appears. This might open the way to laser cooling calcium towards quantum degeneracy and lead to dense atomic samples, e.g. for the study of cold collisions.

We gratefully acknowledge the support by the Deutsche Forschungsgemeinschaft under SFB 407 and under SPP 1116.

References

1. M.D. Barrett, J.A. Sauer, M.S. Chapman, Phys. Rev. Lett. **87**, 010404 (2001)
2. T. Weber, J. Herbig, M. Mark, H.C. Nägerl, R. Grimm, Science **299**, 232 (2003)
3. Y. Takasu, K. Maki, K. Komori, T. Takano, K. Honda, M. Kumakura, T. Yabuzaki, Y. Takahashi, Phys. Rev. Lett. **91**, 040404 (2003)
4. H. Katori, M. Takamoto, V.G. Pal'chikov, V.D. Ovsiannikov, Phys. Rev. Lett. **91**, 173005 (2003)
5. J. McKeever, J. Buck, A. Boozer, A. Kuzmich, H. Nägerl, D. Stamper-Kurn, H. Kimble, Phys. Rev. Lett. **90**, 133602 (2003)
6. O. Mandel, M. Greiner, A. Widera, T. Rom, T. Hänsch, I. Bloch, Nature **425**, 937 (2003)
7. D. Schrader, I. Dotsenko, M. Khudaverdyan, Y. Miroshnychenko, A. Rauschenbeutel, D. Meschede, Phys. Rev. Lett. **93**, 150501 (2004)
8. R. Wester, S. Kraft, M. Mudrich, M. Staudt, J. Lange, N. Vanhaecke, O. Dulieu, M. Weidemüller, Appl. Phys. B **79**, 993 (2004)
9. S.J.M. Kuppens, K.L. Corwin, K.W. Miller, T.E. Chupp, C.E. Wieman, Phys. Rev. A **62**, 013406 (2000)
10. H. Wallis, W. Ertmer, J. Opt. Soc. Am. B **6**, 2211 (1989)
11. T. Binnewies, G. Wilpers, U. Sterr, F. Riehle, J. Helmcke, T.E. Mehlstäubler, E.M. Rasel, W. Ertmer, Phys. Rev. Lett. **87**, 123002 (2001)
12. E.A. Curtis, C.W. Oates, L. Hollberg, Phys. Rev. A **64**, 031403(R) (2001)
13. H. Katori, T. Ido, Y. Isoya, M. Kuwata-Gonokami, Phys. Rev. Lett. **82**, 1116 (1999)
14. U. Sterr, C. Degenhardt, H. Stoehr, C. Lisdat, H. Schnatz, J. Helmcke, F. Riehle, G. Wilpers, C. Oates, L. Hollberg, C. R. Phys. **5**, 845 (2004)
15. R. Maruyama, R.H. Wynar, M.V. Romalis, A. Andalkar, M.D. Swallows, C.E. Pearson, E.N. Fortson, Phys. Rev. A **68**, 011403 (2003)
16. N. Beverini, F. Giammanco, E. Maccioni, F. Strumia, G. Vissani, J. Opt. Soc. Am. B **6**, 2188 (1989)
17. J. Dalibard, C. Cohen-Tannoudji, J. Opt. Soc. Am. B **6**, 2023 (1989)
18. C.N. Cohen-Tannoudji, Rev. Mod. Phys. **70**, 707 (1998)
19. R. Grimm, M. Weidemüller, Y.B. Ovchinnikov, Adv. At. Mol. Opt. Phys. **42**, 95 (2000)
20. S. Chu, J.E. Bjorkholm, A. Ashkin, A. Cable, Phys. Rev. Lett. **57**, 314 (1986)
21. C. Degenhardt, H. Stoehr, U. Sterr, F. Riehle, C. Lisdat, Phys. Rev. A **70**, 023414 (2004)
22. R.C. Hilborn, Am. J. Phys. **50**, 982 (1982), and erratum in: Am. J. Phys. **51**, 471 (1983)
23. A.R. Edmonds, *Angular momentum in quantum mechanics* (Princeton University Press, Princeton, New Jersey, 1957)
24. F. Diedrich, J.C. Bergquist, W.M. Itano, D.J. Wineland, Phys. Rev. Lett. **62**, 403 (1989)
25. N. Masuhara, J.M. Doyle, J.C. Sandberg, D. Kleppner, T.J. Greytak, H.F. Hess, G.P. Kochanski, Phys. Rev. Lett. **61**, 935 (1988)
26. K.B. Davis, M.O. Mewes, M.A. Joffe, M.R. Andrews, W. Ketterle, Phys. Rev. Lett. **74**, 5202 (1995), and erratum: Phys. Rev. Lett. **75**, 2909 (1995)
27. P. Ahmadi, B.P. Timmons, G.S. Summy, Phys. Rev. A **72**, 023411 (2005)
28. K.M. O'Hara, S.R. Granade, M.E. Gehm, T.A. Savard, S. Bali, C. Freed, J.E. Thomas, Phys. Rev. Lett. **82**, 4204 (1999)
29. H. Katori, T. Ido, M. Kuwata-Gonokami, J. Phys. Soc. Jap. **68**, 2479 (1999)
30. P.F. Griffin, K.J. Weatherill, S.G. MacLeod, R.M. Potvliege, C.S. Adams, New J. Phys. **8**, 11 (2006)
31. U. Sterr, C. Degenhardt, H. Stoehr, G. Wilpers, T. Binnewies, F. Riehle, J. Helmcke, C. Lisdat, E. Tiemann, *Ultracold Calcium Atoms for Optical Clocks and Collisional Studies*, in *Proceedings of the XVI International Conference on Laser Spectroscopy*, edited by P. Hannaford, A. Sidorov, H. Bachor, K. Baldwin (World Scientific, New Jersey, 2004), pp. 37–39
32. P.D. Lett, W.D. Phillips, S.L. Rolston, C.E. Tanner, R.N. Watts, C.I. Westbrook, J. Opt. Soc. Am. B **6**, 2084 (1989)
33. M. Gehm, K. O'Hara, T. Savard, J. Thomas, Phys. Rev. A **58**, 3914 (1998)
34. P. Staanum, S.D. Kraft, J. Lange, R. Wester, M. Weidemüller, Phys. Rev. Lett. **96**, 023201 (2006)
35. N. Zahzam, T. Vogt, M. Mudrich, D. Comparat, P. Pillet, Phys. Rev. Lett. **96**, 023202 (2006)